


Computational analysis of obstructive disease and cough intensity effects on the mucus transport and clearance in an idealized upper airway model using the volume of fluid method

Cite as: Phys. Fluids **33**, 021903 (2021); <https://doi.org/10.1063/5.0037764>

Submitted: 19 November 2020 . Accepted: 27 December 2020 . Published Online: 09 February 2021

 Hang Yi (易航),  Qingsheng Wang (汪庆升), and  Yu Feng (冯宇)

COLLECTIONS

 This paper was selected as Featured



View Online



Export Citation



CrossMark

ARTICLES YOU MAY BE INTERESTED IN

[Can face masks offer protection from airborne sneeze and cough droplets in close-up, face-to-face human interactions?—A quantitative study](#)

Physics of Fluids **32**, 127112 (2020); <https://doi.org/10.1063/5.0035072>

[Pressure distribution and flow dynamics in a nasal airway using a scale resolving simulation](#)

Physics of Fluids **33**, 011907 (2021); <https://doi.org/10.1063/5.0036095>

[Fluid dynamics and epidemiology: Seasonality and transmission dynamics](#)

Physics of Fluids **33**, 021901 (2021); <https://doi.org/10.1063/5.0037640>

Physics of Fluids

SPECIAL TOPIC: Tribute to
Frank M. White on his 88th Anniversary

SUBMIT TODAY!



Computational analysis of obstructive disease and cough intensity effects on the mucus transport and clearance in an idealized upper airway model using the volume of fluid method

Cite as: Phys. Fluids **33**, 021903 (2021); doi: [10.1063/5.0037764](https://doi.org/10.1063/5.0037764)

Submitted: 19 November 2020 · Accepted: 27 December 2020 ·

Published Online: 9 February 2021






View Online



Export Citation



CrossMark

Hang Yi (易航),¹  Qingsheng Wang (汪庆升),²  and Yu Feng (冯宇)^{1,a)} 

AFFILIATIONS

¹School of Chemical Engineering, Oklahoma State University, Stillwater, Oklahoma 74078, USA

²Artie McFerrin Department of Chemical Engineering, Texas A&M University, College Station, Texas 77843, USA

^{a)} Author to whom correspondence should be addressed: yu.feng@okstate.edu

ABSTRACT

This study provides a quantitative analysis to investigate the effects of cough intensity and initial mucus thickness on the mucus transport and clearance in a mouth-to-trachea airway geometry using an experimentally validated Volume of Fluid (VOF) based multiphase model. In addition, the accuracy of simplifying mucus as Newtonian fluid is also quantified by the comparisons of mucus transport and clearance efficiencies with the simulations using realistic shear-thinning non-Newtonian fluid viscosities as a function of shear rate. It proves that the VOF model developed in this study can capture air-mucus interface evolution and predict the mucus transport behaviors driven by the expiratory cough waveforms. Numerical results show that noticeable differences can be identified between the simulations using simplified Newtonian fluid and the realistic non-Newtonian fluid viscosity models, which indicates that an appropriate non-Newtonian fluid model should be applied when modeling mucus transport to avoid the possible inaccuracy induced by the Newtonian fluid simplification. Furthermore, the results also indicate that an intense cough can enhance the mucus clearance efficiency in chronic obstructive pulmonary disease (COPD) upper airways. Additionally, although higher mucus clearance efficiency is observed for severe COPD conditions with a thicker mucus layer, there is a possibility of mucus accumulation and obstruction in the upper airway for such a COPD condition if the cough is not strong enough, which will possibly cause further breathing difficulty. The VOF model developed in this study can be further refined and integrated with discrete phase models to predict the mucus clearance effect on inhaled particles explicitly.

Published under license by AIP Publishing. <https://doi.org/10.1063/5.0037764>

I. INTRODUCTION

The inner surface of the airways is covered by airway mucus,¹ which serves as a highly effective defender to trap inhaled toxicants and clear them out of the human respiratory systems driven by cilia beating motion and cough.^{2–4} Mucus is identified as a non-Newtonian fluid⁵ and presents viscoelastic behaviors^{6,7} and shear-thinning characteristics.^{8,9} It has been observed that shear stress between air and mucus is proportional to the square of the airflow rate in the lung airways.¹⁰ In a healthy lung, the mucus thickness is between 2 μm and 50 μm in the trachea and ~ 7 μm in the conducting airways.^{11–16} However, with chronic obstructive pulmonary disease (COPD), mucus will be hyper-secreted, leading to impaired clearance efficiency for inhaled particles and pathogens.¹⁵ Specifically, the hyper-secretion results in increased mucus viscosity and thickness, which can

potentially block the airway, reduce the gas exchange efficiency, and increase the resistance of mucus to be cleared by coughs.^{7,8,17–29} The mucus viscosity in the diseased lung can range from 0.01 Pa s to 100 Pa s with shear-thinning characteristics.^{7,30–37}

Research efforts have been made to study the mucus movement and clearance in simplified and idealized human upper airways using both experiments and computational studies. Qualitative studies have identified that airflow rates, mucus layer thickness, and viscosity are the essential factors affecting mucus clearance in the pulmonary airways.^{10,37,38} It has been proved that high expiratory airflow rates can overcome the viscous resistance and gravity and clear the mucus out more effectively.^{37,39–42} Although experiments have been carried out to investigate the mechanism of mucus clearance driven by airflow in straight tubes to approximate the trachea,^{37,41–44} it is still

challenging to perform such investigations in physiologically realistic airway replicas due to the geometric complexity. To address the knowledge gap mentioned above in geometries with realistic airway anatomy, the Volume of Fluid (VOF) methods and Eulerian wall film model have been employed to track both air and mucus phases.^{17,39,40} Specifically, Paz *et al.*⁴⁰ employed a transient three-dimensional (3D) VOF model to study the mucus movement and clearance in both a straight tube and a subject-specific trachea model. They found that an oscillating airflow would enhance clearance by up to 5% more than a steady-state airflow in the straight tube and in the trachea. Simplifying mucus as a Newtonian fluid, Rajendran and Banerjee³⁹ employed a VOF model and simulated steady-state expiration of air–mucus two-phase flow in an idealized bifurcating geometry, representing generation 0 (G0) to generation 2 (G2). They discovered that Dean's flow in the bifurcations could lead to non-uniform mucus thickness distributions. Other than using the VOF method, Ren *et al.*¹⁷ employed the Eulerian wall film model and found that mechanical ventilation techniques can significantly improve the mucus flow clearance efficiency compared to spontaneous coughing.

However, many vital questions have not been answered, i.e., (1) Will simplifying the mucus as a Newtonian fluid significantly impact the mucus movement and clearance predictions compared with using the more realistic non-Newtonian fluid properties? (2) How do COPD-induced variations in mucus thickness and viscosity influence the cough-driven mucus movement and clearance efficiency?

To partially answer the above-mentioned questions, this study employed an experimentally validated 3D VOF model to predict the cough-driven mucus transport and clearance in an idealized upper airway model from the mouth to trachea. Specifically, the $k-\omega$ transitional Shear Stress Transport (SST) model has been employed in this

study to capture the laminar-to-turbulence flow patterns. To investigate the impacts of mucus viscosity, mucus thickness, and cough intensity on mucus transport and clearance, both Newtonian and non-Newtonian viscosity models were used. Specifically, two different mucus thicknesses, i.e., 1.0 mm and 0.5 mm, were employed, representing different severities of the COPD conditions. Furthermore, two cough waveforms with different average flow rates were used, and the resultant mucus movements and clearances were compared.

II. NUMERICAL METHOD

A. Geometry and mesh

To unveil the underlying fluid dynamics of disease-specific air–mucus flows with different mucus thicknesses σ , two idealized mouth-to-trachea (MT) models [see Figs. 1(a)–1(c)] were created based on the upper airway model used in existing experimental and numerical studies.^{45,46} Different mucus thicknesses represent different COPD severities ($\sigma = 1.0$ mm and $\sigma = 0.5$ mm), i.e., GOLD I and GOLD II, respectively.^{4,37,40} To comprehensively analyze the regional mucus transport behaviors under various cough and disease conditions, the MT model is divided into three different zones, i.e., zone 1 (Z-1), zone 2 (Z-2), and zone 3 (Z-3) [see Fig. 1(a)]. Specifically, Z-1 covers the trachea region, Z-2 represents the region from the glottis to the soft palate, and Z-3 contains the region from the soft palate to the mouth opening.

For the computational mesh, poly-hexcore meshes were generated using Ansys Fluent Meshing (Ansys Inc., Canonsburg, PA). Mesh details for the two MT models are shown in Table I and in Figs. 1(b) and 1(c). Grid sensitivity was investigated by the comparisons of non-dimensionalized velocity profiles \bar{V} at the selected lines, i.e., A–A' and B–B', with an inhalation airflow rate 27.5 ml/s at the mouth opening

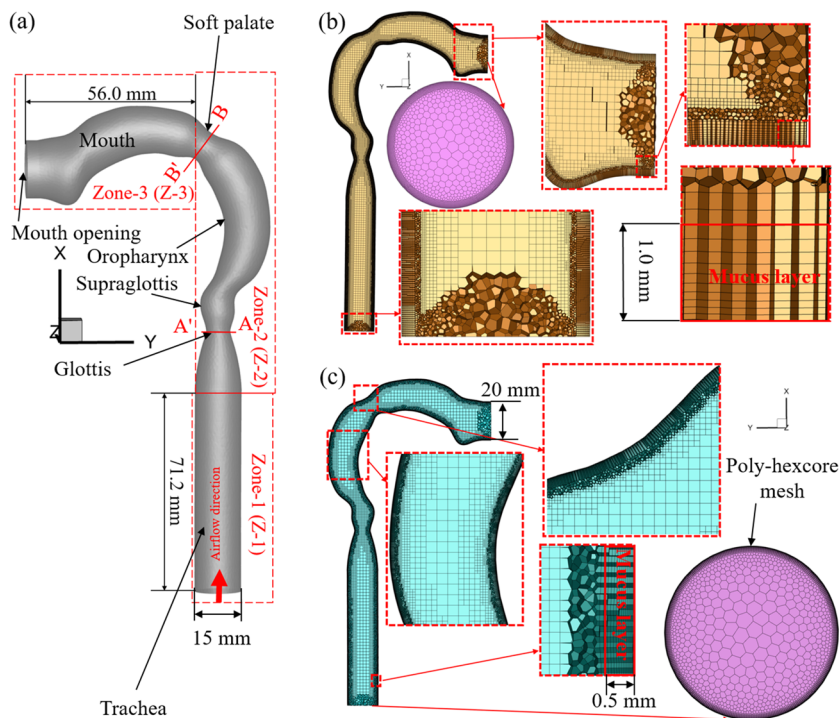


FIG. 1. Schematic of the computational domain with the hybrid mesh details in the two mouth-to-trachea (MT) upper airway models with different mucus thicknesses: (a) Schematic of the MT upper airway geometry. (b) Mesh details of the MT upper airway geometry with $\sigma = 1.0$ mm. (c) Mesh details of the MT upper airway geometry with $\sigma = 0.5$ mm.

[see Figs. 2(a) and 2(b)].⁴⁵ Using different meshes (see Table I), the comparisons between the nondimensionalized velocity magnitude V^* along lines A–A' and B–B' are shown in Figs. 2(a) and 2(b). It can be observed that mesh 1 and mesh 4 are too coarse to obtain accurate results. The variations in simulated velocity profiles are within 1.0% between mesh 2 and mesh 3 and between mesh 5 and mesh 6 [see Figs. 2(a) and 2(b)]. Thus, mesh 2 and mesh 5 are selected as the final meshes for both MT models with the optimal balance between computational efficiency and accuracy.

B. Governing equations

The Volume of Fluid (VOF) model⁴⁷ can be employed to track the interface of two immiscible fluids, and it has dominant advantages to trace the interface behaviors and capture the changes in surface tension on the interface between mucus flow and airflow.⁴⁸ In this study, air and mucus are considered as the primary phase and the secondary phase, respectively. Air and mucus are assumed to be non-interpenetrating. To track both phases, the mucus volume fraction is defined as

$$\alpha_m = \frac{V_m}{V}, \quad (1)$$

where α_m is the mucus volume fraction, V_m is the mucus volume in a certain mesh cell, and V is the mesh cell volume. The air volume fraction is obtained based on the following constraint:

$$\alpha_a = 1 - \alpha_m. \quad (2)$$

Accordingly, the air–mucus mixture properties can be determined by

$$\rho = \alpha_m \rho_m + \alpha_a \rho_a, \quad (3)$$

$$\mu = \alpha_m \mu_m + \alpha_a \mu_a, \quad (4)$$

where ρ and μ are the mixture density and viscosity, respectively.

It is worth mentioning that existing studies assume mucus as a Newtonian fluid.^{39,40,49,50} However, since mucus is non-Newtonian and a shear-thinning liquid,^{37,41,42} it is unknown whether the Newtonian simplification will induce significant differences in the predictions of mucus transport and clearance. Therefore, to address the above-mentioned gap, this study employed both Newtonian and non-Newtonian mucus viscosity models and compared the differences in the computational fluid dynamics (CFD) simulation results. Specifically, mucus viscosity 7.9 Pa s was employed in this study for the Newtonian fluid simulations.⁴² In addition, a non-Newtonian power-law model was also employed in this study to represent the

more realistic shear-thinning behaviors.^{4,7,17,51,52} Specifically, the non-Newtonian μ_m can be defined as

$$\mu_m = \begin{cases} \mu_{mMin} (\gamma \geq \gamma_{Max}) & (5a) \\ a\gamma^b (\gamma_{Min} < \gamma < \gamma_{Max}) & (5b) \\ \mu_{mMax} (\gamma \leq \gamma_{Min}) & (5c) \end{cases}$$

In Eqs. (5a)–(5c), a is the consistency index (CI), which is the average mucus viscosity, and b is the power-law index, which is equal to -0.85 in this study.¹⁷ In addition, γ_{Min} and γ_{Max} are minimum and maximum shear rates, respectively. The mucus viscosities, i.e., 1.0 Pa s–14.8 Pa s with corresponding minimum and maximum shear rates representing the COPD conditions, were employed to study the non-Newtonian fluid affecting mucus transport behaviors (see Fig. 3).^{7,42}

1. Continuity equation

The continuity equation for the mucus can be given as

$$\rho_m \left(\frac{\partial}{\partial t} \alpha_m + \nabla \cdot (\alpha_m \vec{v}_m) \right) = 0, \quad (6)$$

where \vec{v}_m is the mucus velocity vector and α_m is the mucus volume fraction defined by Eq. (1). Accordingly, the air volume fraction α_a can be determined using Eq. (2).

2. Momentum equation

The momentum equation for the air–mucus mixture is solved and given by

$$\frac{\partial}{\partial t} (\rho \vec{v}) + \nabla \cdot (\rho \vec{v} \vec{v}) = -\nabla p + \nabla \cdot (\mu (\nabla \vec{v} + \nabla \vec{v}^T)) + \rho \vec{g} + \vec{F}_{CSF}, \quad (7)$$

where \vec{v} is the velocity vector, \vec{g} is the gravity vector, and p is the pressure. The mixture density ρ and viscosity μ can be determined by Eqs. (3) and (4). \vec{F}_{CSF} is the surface tension force (CSF), which only applies at the air–mucus interface. Specifically, \vec{F}_{CSF} can be calculated by⁵³

$$\vec{F}_{CSF} = 2\beta \frac{\rho \kappa \vec{n}}{\rho_m + \rho_a}, \quad (8)$$

where β is the surface tension coefficient, which is equal to 0.032 N/m.^{54,55} Specifically, Eq. (8) is based on the CSF method,⁵³ in which the surface curvature κ can be defined as

$$\kappa = \nabla \cdot \hat{n}, \quad (9)$$

TABLE I. Mesh details in the mesh independence tests for air-driven mucus clearance simulations using the VOF model.

Geometry	Mesh	Prism layers	Minimum-size (mm)	Volume-maximum skewness	Volume elements
Upper airway ($\sigma = 1.0$ mm)	Mesh 1	12	0.083	0.61	1 878 487
	Mesh 2 (final)	12	0.05	0.61	6 280 525
	Mesh 3	20	0.05	0.71	9 000 552
Upper airway ($\sigma = 0.5$ mm)	Mesh 4	12	0.083	0.60	1 472 425
	Mesh 5 (final)	15	0.02	0.43	6 785 182
	Mesh 6	30	0.02	0.60	11 735 372

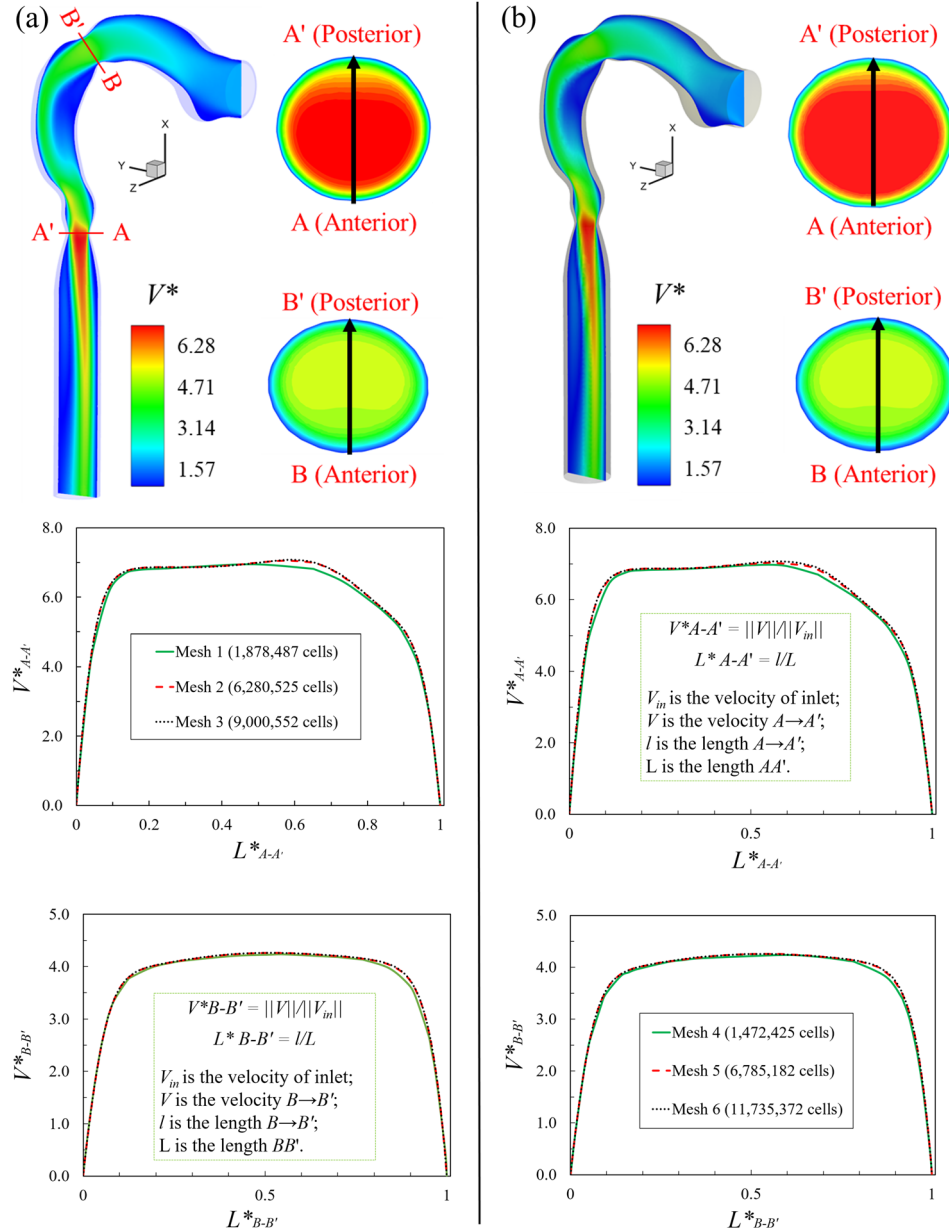


FIG. 2. Mesh independence tests for the two MT models: (a) $\sigma = 1.0$ mm. (b) $\sigma = 0.5$ mm.

$$\vec{n} = \nabla \alpha, \quad (10)$$

$$\hat{n} = \frac{\vec{n}}{|\vec{n}|}, \quad (11)$$

where κ is the surface curvature, \hat{n} is the divergence of the unit normal, α is the volume fraction, and \vec{n} is the gradient of the volume fraction.

To better model the surface curvature κ in Eq. (9) where the mucus layer is very thin, the effects of wall adhesion at the air–mucus interface is considered in terms of the equilibrium contact angle θ_w between the fluid and the airway wall.⁵⁶ The contact angle θ_w is used to correct the surface normal vectors of the near-wall mesh cell faces,⁵³ which is given by

$$\hat{n} = \hat{n}_w \cos \theta_w + \hat{t}_w \sin \theta_w, \quad (12)$$

where \hat{n}_w and \hat{t}_w are unit normal and tangential vectors to the wall, respectively.

C. Mucus clearance efficiency

To calculate the mucus clearance efficiency η_{ce} , the definition in a previous study is employed,⁴⁰ i.e.,

$$\eta_{ce} = -\frac{\Delta V_m}{V_{m,ini}} \times 100\%, \quad (13)$$

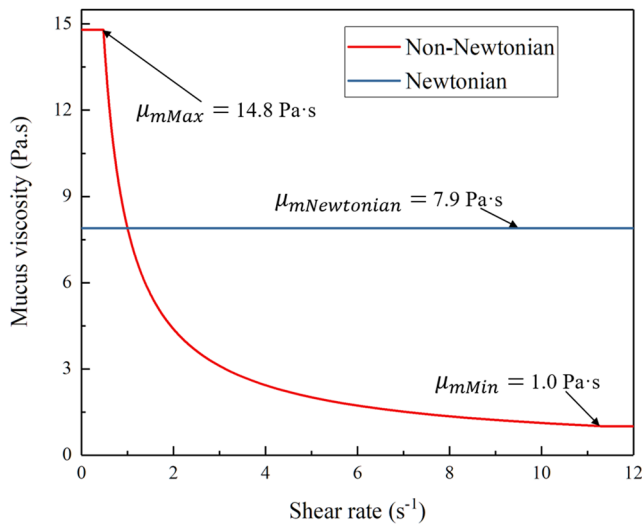


FIG. 3. Newtonian and non-Newtonian mucus viscosities employed in this study.

where $V_{m,ini}$ is the initial total mucus volume in the computational domain and ΔV_m is the accumulated mucus volume change.

D. Boundary and initial conditions

1. Inlet boundary conditions with transient cough wave

Two transient cough waveforms were applied as the inlet boundary conditions at the trachea opening (see Fig. 4), representing the expiratory conditions. Specifically, to study cough strength (CS) effects on mucus movement and clearance in the upper airway, two different transient cough waveforms were employed with different averaged flow rates (see Fig. 4). As shown in Fig. 4, the waveform of CS-I is based on the measurements of 25 human subjects,^{57–59} and it has been employed in previous studies.^{60–63} The other waveform, CS-II, was

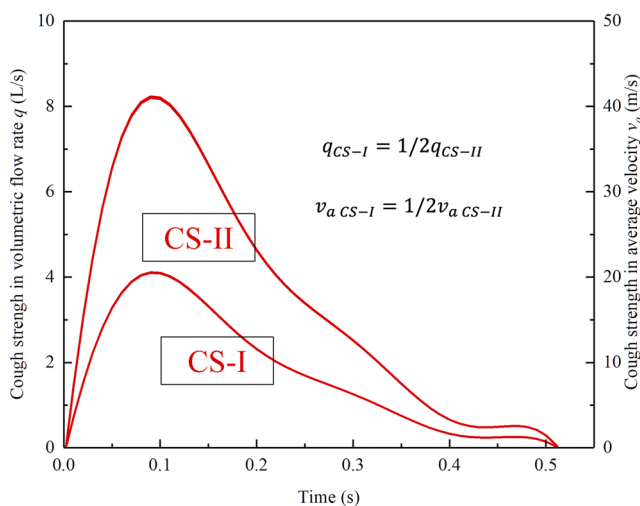


FIG. 4. Cough-wave boundary conditions at the COPD upper airways.

generated by amplifying CS-I twice to investigate the cough strength effect on mucus movement and clearance.

2. Airway wall and outlet boundary conditions

The airway walls are assumed to be stationary and non-slip. The gauge pressure at the mouth opening is equal to the atmospheric pressure. Additionally, the backflow direction at the mouth opening is determined based on the direction of the flow in the cell layer adjacent to the mouth opening outlet.⁶⁴

3. Initialization for mucus regions

To represent the existence of a mucus layer at the inner wall of the airways, two mucus thicknesses $\sigma = 0.5$ mm and $\sigma = 1.0$ mm were used to represent two different COPD severities, i.e., GOLD I and GOLD II,^{4,37,40} based on the fact that COPD stages in this work were classified by the high-secreted mucus volume lined to the airway wall, leading to constricted airway lumen and airflow obstructions.⁶⁵ Additionally, the volume fraction α_m in the near-wall region with specific σ was initialized to be equal to 1.0.

4. Numerical setup

VOF simulations were executed using Ansys Fluent 2020 R1 (Ansys Inc., Canonsburg, PA). Simulations in the straight tube for model validations were performed on a local Dell Precision T7910 workstation (Intel® Xeon® Processor E5-2683 v4 with dual processors, 32 cores, and 256 GB RAM); it took ~ 48 h to finish the simulation with the physical time duration 5.0 s. Simulations in the idealized upper airway geometry were ran on the supercomputer “Pete” at the High Performance Computing Center (HPCC) at Oklahoma State University (OSU) (IntelXeon Processor Gold 6130 CPU with dual processors, 32 cores, 64 threads, and 96 GB RAM). In Newtonian fluid simulations, each case took ~ 120 h to compute one cough-wave duration 0.5126 s, while ~ 168 h were spent calculating one case for the non-Newtonian fluid simulations. The Pressure-Implicit with Splitting of Operator (PISO) algorithm was employed for the pressure-velocity coupling, and the least-squares cell-based scheme was applied to calculate the cell gradient. The Pressure Staggering Option (PRESTO!) scheme was employed for pressure discretization. The compressive method was used for the spatial discretization of the volume fraction. In addition, the second-order upwind scheme was applied for the discretization of momentum and turbulent kinetic energy. Convergence is defined for continuity, momentum, and supplementary equations when residuals are lower than 1.0×10^{-3} .

III. RESULTS AND DISCUSSION

A. VOF model validation

To validate the VOF model, mucus thickness, mucus transport velocity, and mucus volume fraction were compared with the experimental data⁴² under different boundary conditions in the 3D straight tube (see the [supplementary material](#) for the geometry and mesh details). In the simulations for model validation, the mucus feeding rate $q_m = 1$ ml/min, and the airflow rate $q_a = 19.5$ ml/min. The steady state was considered achieved when the mucus feed rate in the straight tube became equal to the mucus outflow rate. Dependent variables

employed in the validation (see Fig. 5) are defined as follows. The mean mucus layer transport velocity \bar{v}_m is defined as

$$\bar{v}_m = \frac{4q_m}{\pi D^2} \left(1 - \left(1 - \frac{2\sigma}{D} \right)^2 \right)^{-1}, \quad (14)$$

where q_m is the mucus feeding rate and D is the straight tube diameter. Equation (14) can be simplified with the function of mucus volume fraction α_m as follows:

$$\bar{v}_m = \frac{4q_m}{\pi D^2 \alpha_m}, \quad (15)$$

$$\sigma = \frac{D}{2} \left(1 - (1 - \alpha_m)^{-0.5} \right). \quad (16)$$

As shown in Figs. 5(a)–5(c), except for the relative error of the mucus transport velocity \bar{v}_m , which is $\sim 8\%$ between simulations and experiments,⁴² the relative errors of mean mucus layer thickness σ and mucus volume fraction α_m are both less than 5%. With good agreement compared with the experimental data, the capability of the VOF

model is validated to predict mucus movement behaviors in this study.

B. Newtonian vs non-Newtonian mucus viscosity models

To investigate whether using the simplified Newtonian fluid model will induce significant differences in mucus transport and clearance, the CFD results are compared using Newtonian fluid and non-Newtonian fluid models. Specifically, Figs. 6 and 7 manifest noticeable differences between Newtonian fluid (7.9 Pa s) and non-Newtonian fluid (1.0 Pa s–14.9 Pa s) in calculations of the mucus clearance efficiency η_{ce} in the different zones of the MT model. It shows that the non-Newtonian fluid simulations provide higher mucus clearance efficiency than the Newtonian fluid simulations with the same cough strengths and mucus thicknesses. Such an observation is consistent with the perspectives from previous studies that pseudoplastic non-Newtonian fluids with shear-thinning behavior can transport more efficiently than Newtonian fluids.^{66–69} This conclusion can also be

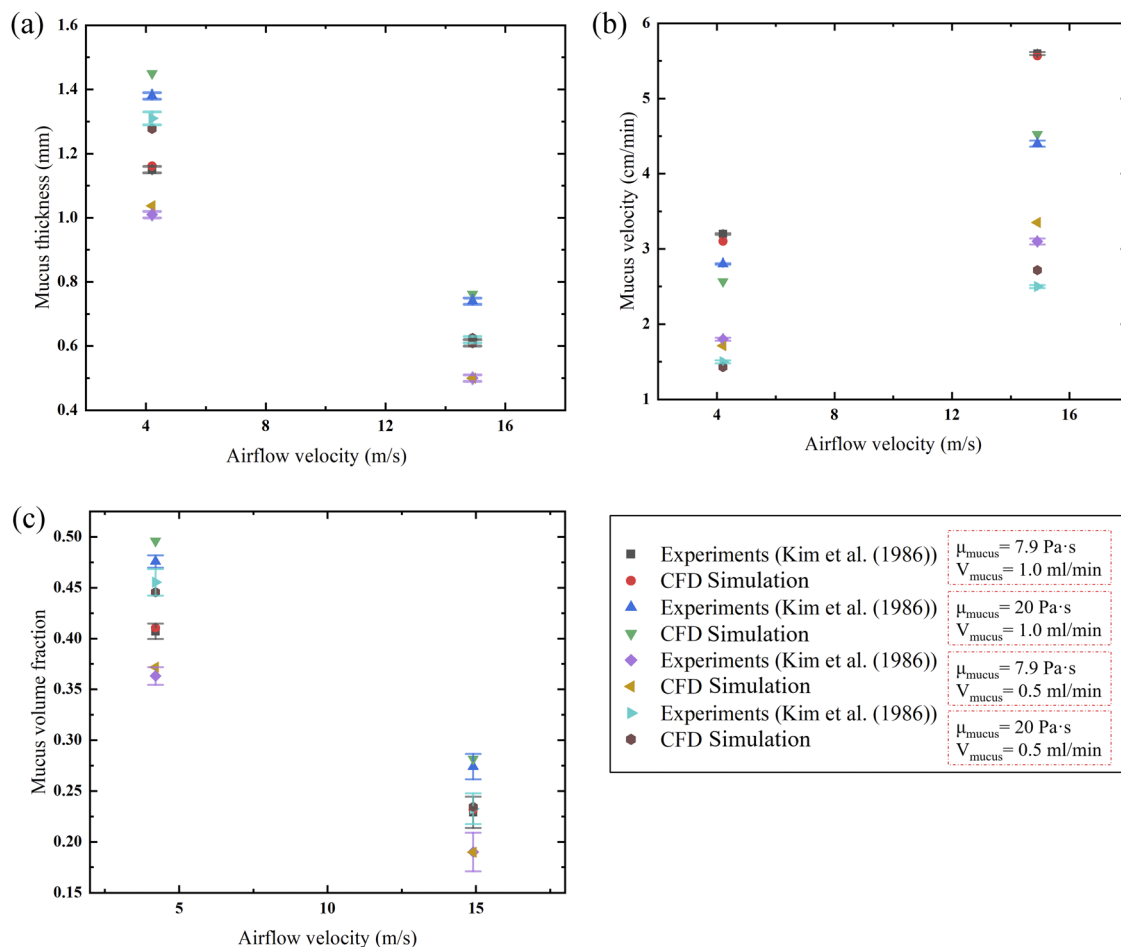


FIG. 5. Comparison of computational results for a straight tube with experimental data (Kim, Greene *et al.*, 1986).⁴² (a) Relationship between the mucus thickness and the airflow velocity. (b) Relationship between the mucus velocity and the airflow velocity. (c) Relationship between the mucus volume fraction and the airflow velocity.

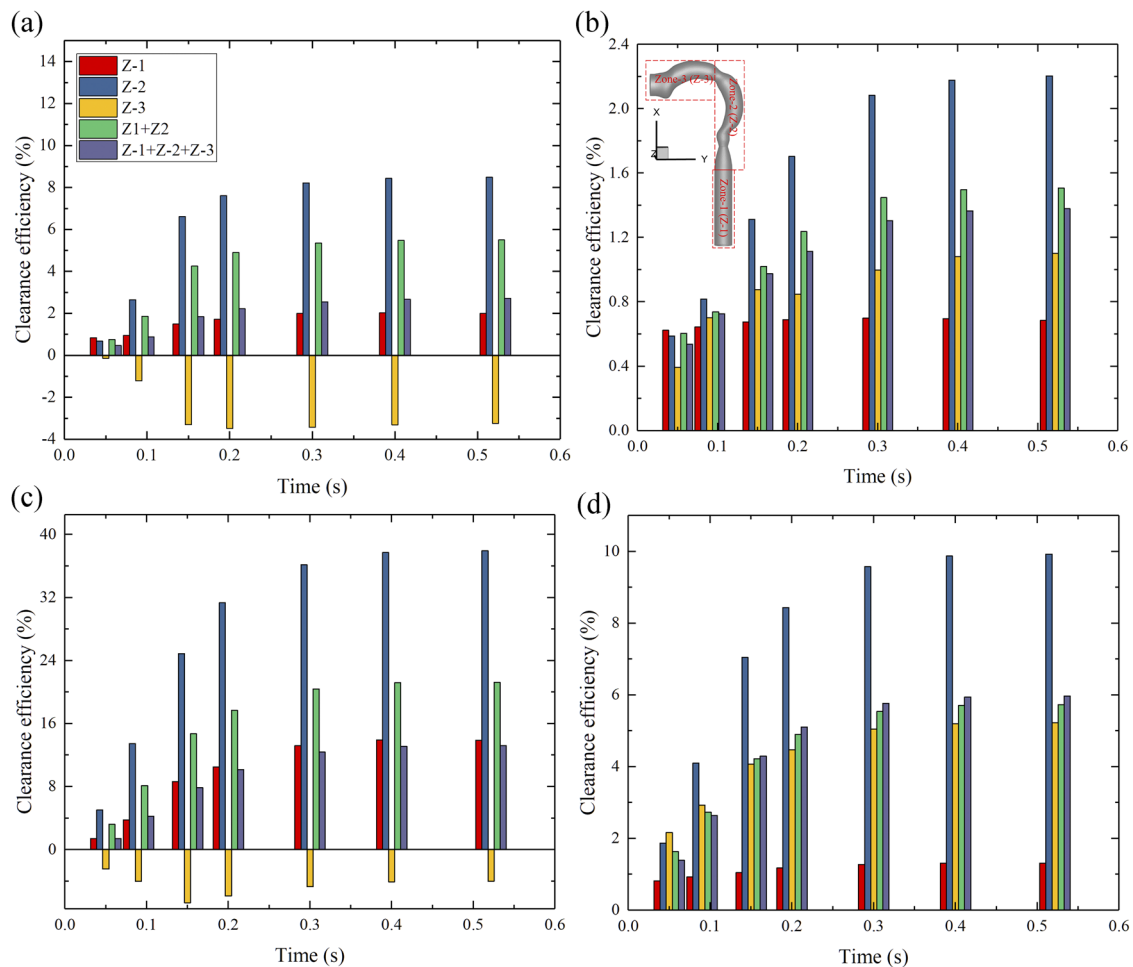


FIG. 6. Mucus clearance efficiency in the MT model with Newtonian mucus under different conditions: (a) CS-I and $\sigma = 1.0$ mm. (b) CS-I and $\sigma = 0.5$ mm. (c) CS-II and $\sigma = 1.0$ mm. (d) CS-II and $\sigma = 0.5$ mm.

proved directly not only from the comparisons of mucus clearance efficiency (see Figs. 6 and 7) but also from results based on the average mucus volumetric flow rate \bar{q}_m in a cough wave at selected time stations in the MT models (see Table II). In the non-Newtonian fluid simulations, the clearance efficiency η_{ce} or volumetric flow rate \bar{q}_m is about 3.41 (with CS-II and $\sigma = 1.0$ mm) to 7.80 (with CS-I and $\sigma = 0.5$ mm) times higher than the values with the Newtonian fluid (see Tables II and III). Similarly, regional clearance efficiencies in Z-1, Z-2, Z-3, and Z-1 + Z-2 (see Figs. 6 and 7) demonstrate that mucus can be transported faster by the cough-driven airflow using the non-Newtonian power-law model, which exhibits a proportional increase in the shear rate as a function of shear stress.⁷⁰ It should be noted that mucus accumulation appears in local region Z-3 in both Newtonian and non-Newtonian fluid simulations. In non-Newtonian fluid simulations with the shear-thinning properties, mucus accumulation is slower and mucus transport is faster than in Newtonian fluid simulations (see Figs. 6 and 7).

These phenomena can be explained based on comparisons between the velocity profiles and vectors and mucus transport

characteristics in the MT model (see Figs. 8–15). Nondimensionized velocity magnitude V^* and mucus volume fraction α_m variations near the air–mucus interfaces at cross sections C–C' and D–D' are enlarged and shown in Figs. 8 and 9. Using the iso-surfaces $\alpha_m = 0.01$, the air–mucus interfaces are visualized in Figs. 10 and 12–14. Accordingly, the velocities in the mucus phase with $0.01 \leq \alpha_m \leq 1$ were employed to calculate the average mucus movement velocity \bar{v}_m . \bar{v}_m at different sides of the cross sections C–C' and D–D' are listed in Table IV. As shown by the comparisons between non-Newtonian fluid and Newtonian fluid (CS-I and $\sigma = 1.0$ mm) at the locations near C and C' sides [I and II in Fig. 8(a)] at $t = 0.05$ s, \bar{v}_m in the non-Newtonian fluid simulations are ~ 0.1106 m/s and 1.2277 m/s, while \bar{v}_m in the Newtonian fluid simulations are much lower, i.e., 0.0029 m/s and 0.1739 m/s at corresponding sides. The above-mentioned comparison indicates that the mucus near the air–mucus interface can be cleared more than three times faster than the Newtonian fluid at this time location [see Fig. 8(a) and Table IV]. Using the Newtonian fluid property may underpredict the mucus clearance efficiency with significant errors. The velocity vectors shown in Figs. 12 and 13 indicate that the

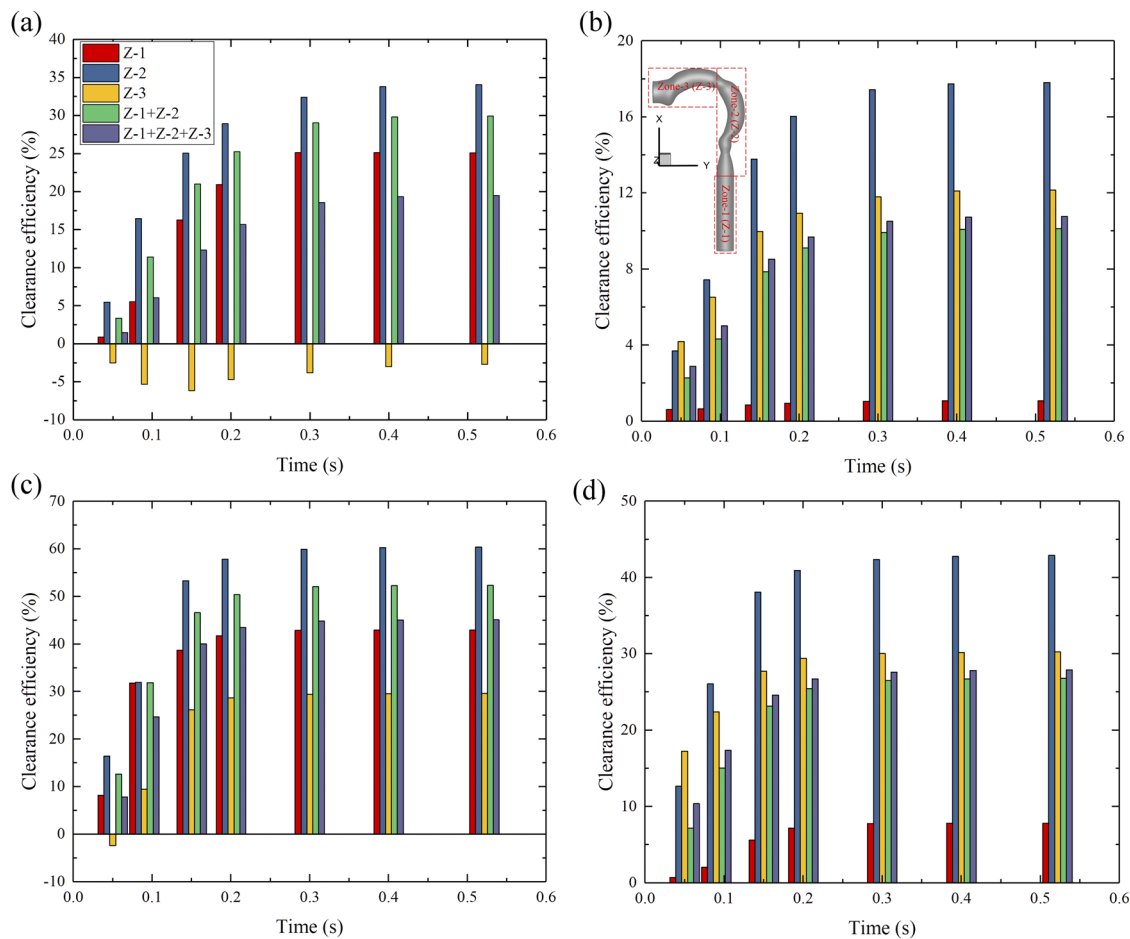


FIG. 7. Mucus clearance efficiency in the MT model with non-Newtonian mucus under different conditions: (a) CS-I and $\sigma = 1.0$ mm. (b) CS-I and $\sigma = 0.5$ mm. (c) CS-II and $\sigma = 1.0$ mm. (d) CS-II and $\sigma = 0.5$ mm.

changes in mucus transport characteristics can lead to different secondary flow patterns. Specifically, the highlighted regions in Figs. 12 and 13 show that stronger secondary flows are developed in the non-Newtonian fluid with shear-thinning behaviors, which can assist in

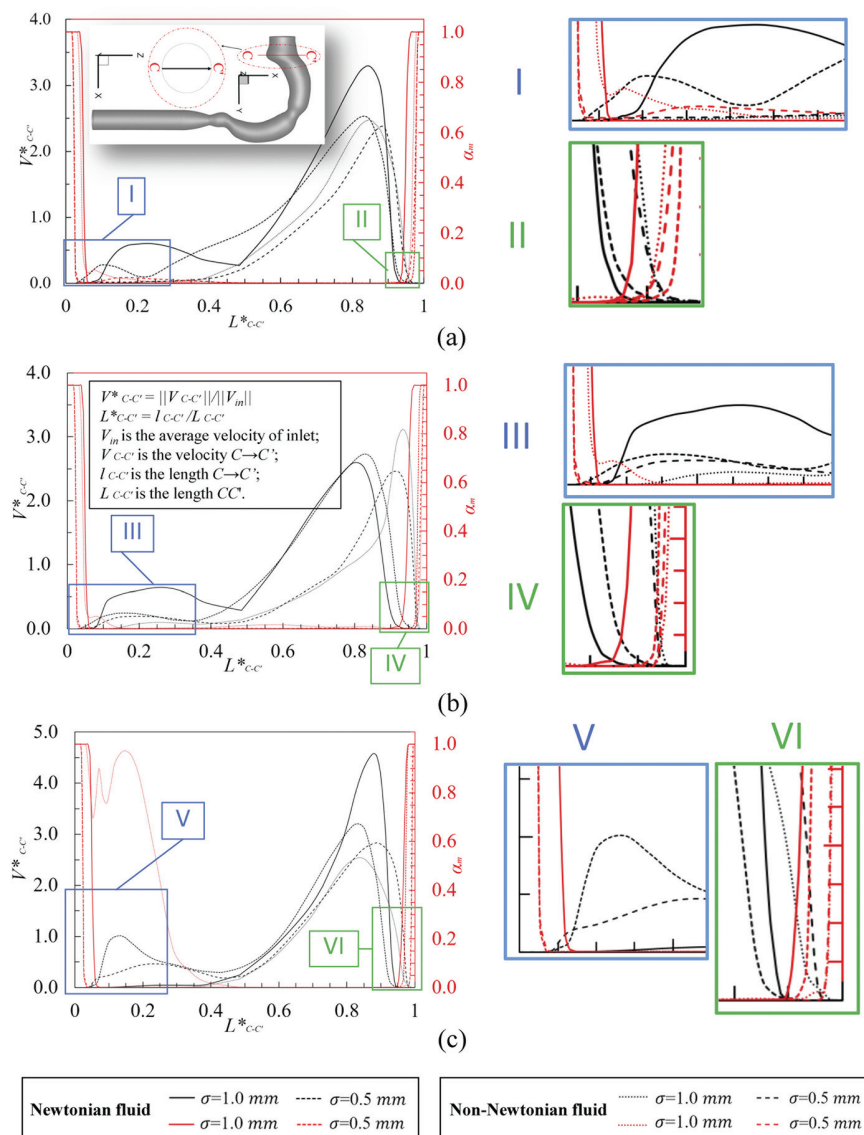
clearing the mucus faster than Newtonian fluid.⁷¹ Similarly, the comparable results of average mucus movement velocity \bar{v}_m at the locations close to both D and D' sides have been obtained under corresponding cough strength and mucus thickness between

TABLE II. Average volumetric flow rate \bar{q}_m (ml/s) at the selected time stations during a single cough.

Conditions			Time (s)						
Mucus thickness (mm)	Mucus viscosity (Pa s)	Cough strength	0.05	0.09	0.15	0.20	0.30	0.40	0.5126
1.0	7.9	CS-I	1.05	1.11	1.38	1.25	0.96	0.76	0.60
	1–14.8	CS-I	3.34	7.64	9.30	8.88	7.01	5.47	4.31
	7.9	CS-II	3.20	5.35	5.94	5.76	4.67	3.72	2.92
	1–14.8	CS-II	17.73	31.10	30.25	24.61	16.92	12.75	9.96
0.5	7.9	CS-I	0.58	0.43	0.35	0.30	0.24	0.19	0.15
	1–14.8	CS-I	3.14	3.03	3.09	2.63	1.90	1.46	1.14
	7.9	CS-II	1.77	1.65	1.53	1.33	1.00	0.76	0.60
	1–14.8	CS-II	11.27	10.49	8.92	7.26	5.00	3.78	2.96

TABLE III. Mucus clearance efficiency (%) at selected time stations during a single cough.

Conditions			Time (s)						
Mucus thickness (mm)	Mucus viscosity (Pa s)	Cough strength	0.05	0.09	0.15	0.20	0.30	0.40	0.5126
1.0	7.9	CS-I	0.46	0.88	1.84	2.22	2.55	2.67	2.71
	1–14.8		1.48	6.67	12.32	15.68	18.56	19.33	19.50
	7.9	CS-II	1.41	4.25	7.86	10.17	12.38	13.12	13.20
	1–14.8		7.83	24.71	40.07	43.47	44.82	45.03	45.08
0.5	7.9	CS-I	0.54	0.73	0.97	1.11	1.30	1.37	1.38
	1–14.8		2.89	5.02	8.52	9.69	10.51	10.73	10.77
	7.9	CS-II	1.63	2.73	4.22	4.90	5.54	5.70	5.73
	1–14.8		10.36	17.37	24.61	26.71	27.62	27.82	27.90

**FIG. 8.** Nondimensionalized velocity profiles and mucus volume fraction at the cross section C-C' computed with CS-I and mucus properties at different time stations in a cough wave: (a) $t = 0.05$ s; (b) $t = 0.09$ s; and (c) $t = 0.40$ s.

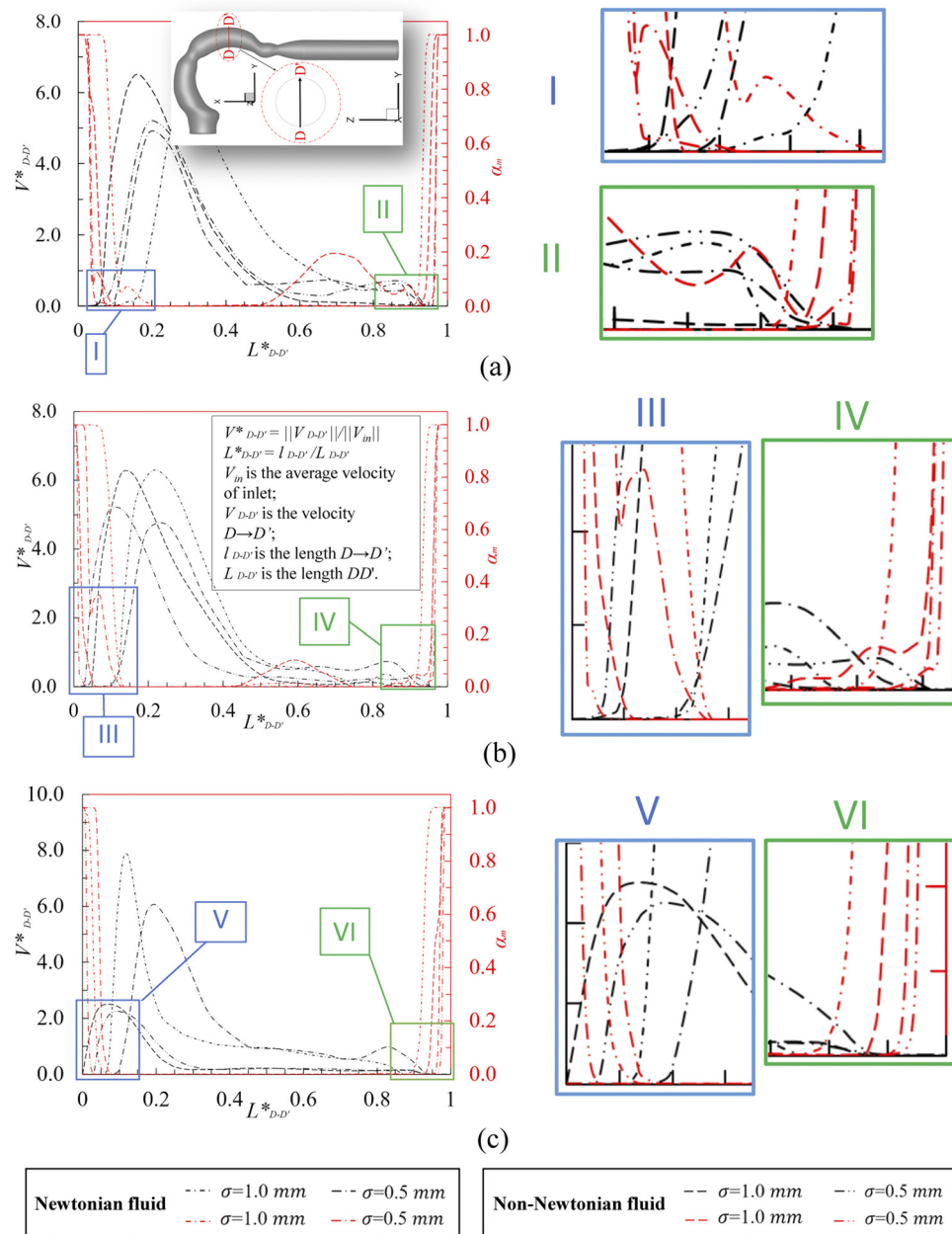


FIG. 9. Nondimensionalized velocity profiles V^* and mucus volume fraction α_m at the cross section D-D' computed with CS-II and mucus properties at different time stations in a cough wave: (a) $t = 0.05 \text{ s}$; (b) $t = 0.09 \text{ s}$; and (c) $t = 0.40 \text{ s}$.

non-Newtonian fluid and Newtonian fluid at time stations, i.e., $t = 0.05 \text{ s}$ and 0.09 s , shown in Figs. 9(a) and 9(b) and in Table IV. Moreover, a non-Newtonian mucus velocity is lower than the simulation results with the Newtonian mucus simplifications [see Fig. 9(c) and Table IV] under stronger cough strength (CS-II) at $t = 0.40 \text{ s}$. This is due to the more dominant viscous dissipation effect of the airway wall boundaries with the thinner mucus layer in non-Newtonian simulations [see Fig. 9(c)].⁷²

In summary, significant differences between the simulations using idealized Newtonian fluid and realistic non-Newtonian fluid viscosities were observed in mucus clearance efficiency and characteristics in the upper airways. To avoid possible errors induced by the Newtonian fluid simplification, it is highly recommended to employ non-Newtonian fluid models [see Eqs. (5a)–(5c)] instead of the simplified Newtonian fluid viscosity model when modeling mucus movement behaviors in upper airway computational domains. Since it has

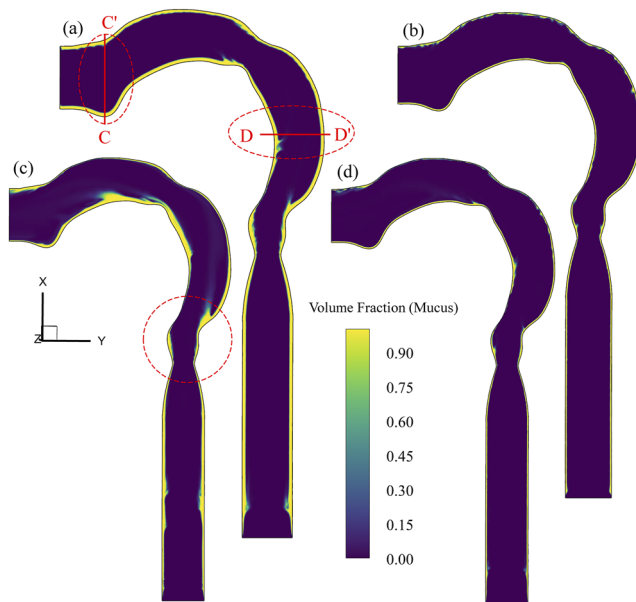


FIG. 10. Mucus distributions in the sagittal plane ($Z = 0$) with CS-I at $t = 0.09$ s with different mucus thicknesses and mucus rheological properties: (a) $\sigma = 1.0$ mm with Newtonian fluid; (b) $\sigma = 0.5$ mm and Newtonian fluid; (c) $\sigma = 1.0$ mm and non-Newtonian fluid; and (d) $\sigma = 0.5$ mm and non-Newtonian fluid.

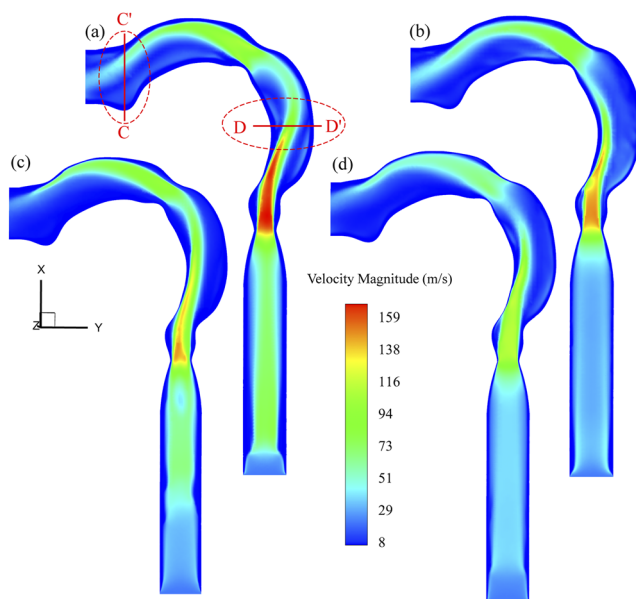


FIG. 11. Velocity magnitudes in the sagittal plane ($z = 0$) with CS-I at $t = 0.09$ s (cough-wave peak) under different mucus thicknesses and mucus rheological properties: (a) $\sigma = 1.0$ mm with Newtonian fluid; (b) $\sigma = 0.5$ mm and Newtonian fluid; (c) $\sigma = 1.0$ mm and non-Newtonian fluid; and (d) $\sigma = 0.5$ mm and non-Newtonian fluid.

been confirmed in this section that the non-Newtonian fluid simulations are more realistic and accurate, we would like to focus on the discussions based on non-Newtonian fluid simulation results in Secs. III C–III E for parametric analyses.

C. Effects of mucus thickness

Two mucus thicknesses $\sigma = 1.0$ mm and $\sigma = 0.5$ mm were employed in this study to morphologically represent two COPD levels, i.e., GOLD I and GOLD II (see Fig. 1) for investigating the mucus thickness effects on mucus clearance efficiency and transport behaviors. Specifically, the simulation results in mucus clearance efficiency in different regions (see Fig. 7), average mucus transport velocities (see Figs. 8 and 9), velocity magnitudes at the sagittal plane ($Z = 0$) [see Figs. 11(c), 11(d), 15(c), and 15(d)], and mucus characteristics in representative local regions (see Fig. 16) are compared. Figures 7(a) and 7(c) show the regional mucus clearance efficiencies (η_{ce}) in the MT model with $\sigma = 1.0$ mm, and Figs. 7(b) and 7(d) show η_{ce} values with $\sigma = 0.5$ mm during a single cough at different time stations. In addition, Table III lists the η_{ce} values at different times and shows that the maximum η_{ce} is 45.08%, which is with strong cough CS-II and $\sigma = 1.0$ mm, and the minimum η_{ce} is 10.77%, which is with mild cough CS-I and $\sigma = 0.5$ mm. Comparisons between Figs. 7(a) and 7(b) demonstrate that with the same cough waveform, CS-I, the upper airway model with thicker mucus generates higher mucus clearance efficiency. A similar observation can be found in the simulations with CS-II [see Figs. 7(c) and 7(d)]. Specifically, with the same cough waveform, η_{ce} in the MT model with $\sigma = 1.0$ mm is about two times of the η_{ce} value in the MT model with $\sigma = 0.5$ mm. The higher η_{ce} is because the average mucus volumetric flow rate \bar{q}_m with $\sigma = 1.0$ mm is ~ 4 times of \bar{q}_m with $\sigma = 0.5$ mm (see Table II). Although when cough strengths are the same, thicker mucus can lead to a smaller lumen for the airflow. The smaller lumen can lead to a higher velocity gradient and shear stress at the air–mucus interfaces [see Figs. 11(c), 11(d), 15(c), and 15(d)]. As an example of the evidence to support the above-mentioned underlying fluid dynamics, the average mucus velocity \bar{v}_m in the upper airway with $\sigma = 1.0$ mm is higher than \bar{v}_m in the simulation results with $\sigma = 0.5$ mm (see Figs. 8 and 9 and Table IV).

It can also be found that the mucus layer thickness varies spatially in different regions (i.e., Z-1, Z-2, and Z-3) during the clearance process driven by the coughs [see Figs. 7(a), 7(c), 10, 14, and 16]. Mucus can be accumulated and entrapped in Z-3 with a more severe COPD level [see R-1 to R-3 in Figs. 16(a) and 16(b)], especially under the condition with CS-I that the clearance efficiencies are negative at all selected time stations (see Fig. 7). Such an accumulation effect in Z-3 is because the mucus in Z-1 and Z-2 can move into Z-3 easily, but not be able to move further to the mouth front due to the combined effect of gravity and low airflow momentum [see Figs. 11(c), 11(d), 15(c), and 15(d)]. In contrast, with $\sigma = 0.5$ mm, the mucus thickness is distributed more evenly and has no distinguished changes in the submandibular region [see R-3 in Figs. 16(c) and 16(d)], which indicates no accumulation of the mucus in Z-3 during the expiratory cough when the COPD condition is not severe.

Moreover, it has been commonly recognized that mucus can be easily spat out from the mouth by moving the oral muscles if mucus can be transported through the throat from the trachea to the oral region.^{73,74} Thus, the total mucus clearance efficiency in Z-1 and Z-2 may be more informative to represent the difficulty in mucus clearance

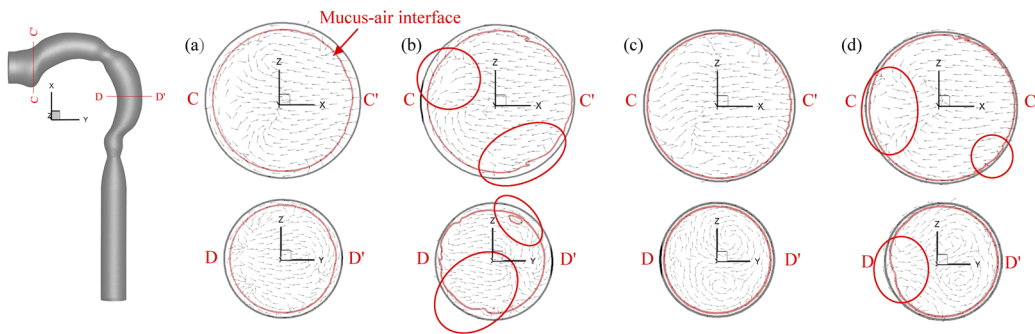


FIG. 12. Velocity vectors in selected planes C-C' and D-D' with CS I at $t = 0.09$ s with different mucus properties: (a) $\sigma = 1.0$ mm with Newtonian fluid; (b) $\sigma = 1.0$ mm and non-Newtonian fluid; (c) $\sigma = 0.5$ mm and Newtonian fluid; and (d) $\sigma = 0.5$ mm and non-Newtonian fluid.

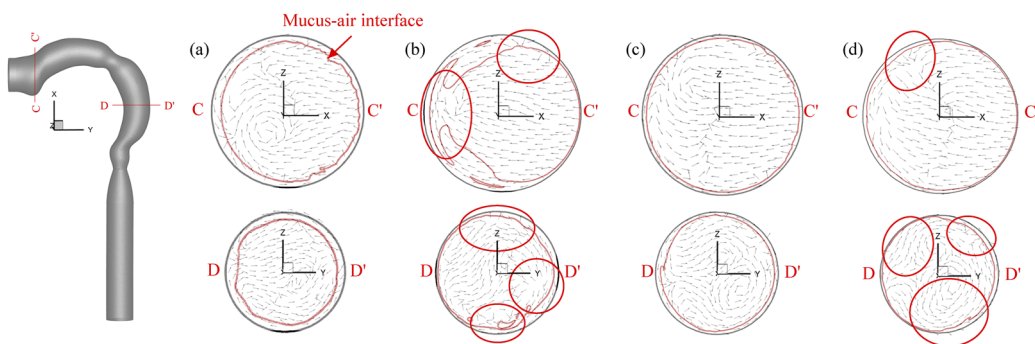


FIG. 13. Velocity vectors in selected planes C-C' and D-D' with CS II at $t = 0.09$ s with different mucus characteristics: (a) $\sigma = 1.0$ mm with Newtonian fluid; (b) $\sigma = 1.0$ mm and non-Newtonian fluid; (c) $\sigma = 0.5$ mm and Newtonian fluid; and (d) $\sigma = 0.5$ mm and non-Newtonian fluid.

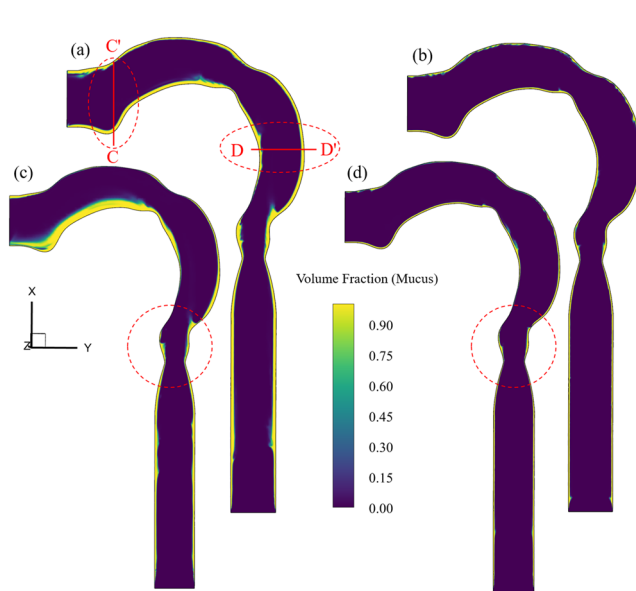


FIG. 14. Mucus distributions in the sagittal plane ($Z = 0$) with CS-I at $t = 0.40$ s under different mucus thicknesses and mucus rheological properties: (a) $\sigma = 1.0$ mm with Newtonian fluid; (b) $\sigma = 0.5$ mm and Newtonian fluid; (c) $\sigma = 1.0$ mm and non-Newtonian fluid; and (d) $\sigma = 0.5$ mm and non-Newtonian fluid.

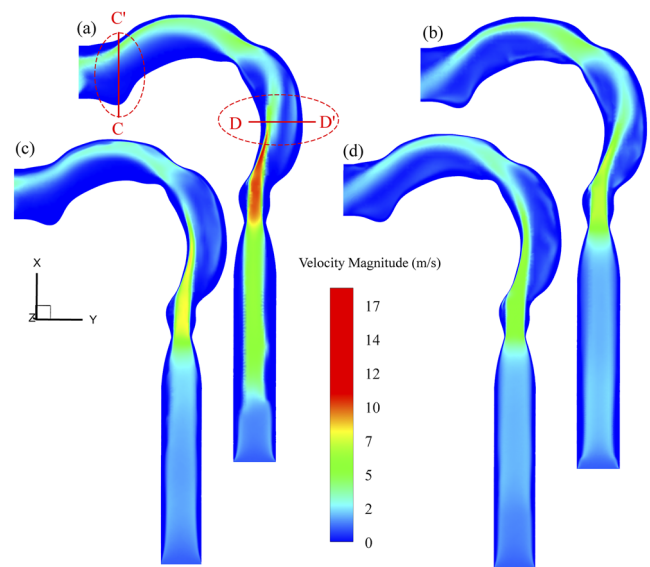


FIG. 15. Velocity magnitudes in the sagittal plane ($z = 0$) with CS-II at $t = 0.40$ s under different mucus thicknesses and mucus rheological properties: (a) $\sigma = 1.0$ mm with Newtonian fluid; (b) $\sigma = 0.5$ mm and Newtonian fluid; (c) $\sigma = 1.0$ mm and non-Newtonian fluid; and (d) $\sigma = 0.5$ mm and non-Newtonian fluid.

TABLE IV. Average mucus velocity \bar{v}_m (m/s) at each across planes C–C' and D–D' at selected time stations.

Conditions				Side of interface at C–C' and D–D'			
Mucus thickness (mm)	Mucus viscosity (Pa s)	Cough strength	Time (s)	C	C'	D	D'
1.0	7.9	CS-I	0.05	0.002 9	0.173 9	0.019 59	0.004 8
			0.09	0.004 7	0.361 0	1.086 4	0.027 4
			0.40	0.000 1	0.001 3	0.003 7	0.000 4
			0.05	0.001 0	1.277 3	2.596 2	0.034 79
			0.09	0.045 67	1.114 1	11.801 6	0.381 4
	1–14.8		0.40	0.029 3	0.073 47	1.032 45	0.006 9
			0.05	0.006 1	1.316 3	8.839 5	0.152 7
			0.09	0.011 7	1.727 1	11.433 3	0.064 09
			0.40	0.077 1	0.08	0.007 5	0.000 7
			0.05	0.152 2	8.580 0	14.832 7	1.021 4
	7.9	CS-II	0.09	0.204 6	0.913 0	8.688 9	0.442 2
			0.40	0.002 4	0.008 0	No mucus	0.007 0
			0.05	0.007 4	0.211 4	0.557 0	0.211 2
			0.09	0.004 0	0.048 0	0.289 3	0.011 1
			0.40	0.000 4	0.000 4	0.001 5	0.000 2
0.5	1–14.8	CS-I	0.05	0.011 9	1.584 2	1.203 8	0.068 2
			0.09	0.017 5	2.270	0.995 1	0.037 5
			0.40	0.000 2	0.005 2	0.006 7	0.003 4
			0.05	0.003 32	1.077 3	0.338 4	0.032 9
			0.09	0.003 8	0.311 9	0.481 3	0.218 2
	7.9	CS-II	0.40	0.000 2	0.004 1	0.006 5	0.000 6
			0.05	0.057 4	3.477 7	2.821 6	0.609 3
			0.09	0.016 6	1.006 1	1.839 1	0.209 0
			0.40	0.000 01	0.000 1	0.000 5	0.000 1
			0.05	0.057 4	3.477 7	2.821 6	0.609 3
	1–14.8		0.09	0.016 6	1.006 1	1.839 1	0.209 0
			0.40	0.000 01	0.000 1	0.000 5	0.000 1
			0.05	0.057 4	3.477 7	2.821 6	0.609 3
			0.09	0.016 6	1.006 1	1.839 1	0.209 0
			0.40	0.000 01	0.000 1	0.000 5	0.000 1

than the entire MT model. However, it is interesting to find that with a mild COPD condition (i.e., $\sigma = 0.5$ mm), the clearance efficiency in the entire MT model is higher than the total of Z-1 and Z-2 [see Figs. 7(b) and 7(d)]. This is because volume of mucus feeding in Z-3 is less than the amount cleared out from this region, implying that the viscosity resistance plays a more significant role in the mucus transport behaviors.

D. Effects of cough strength

Two cough waveforms, i.e., CS-I and CS-II, representing two different cough strengths (see Fig. 4) with the relationship of $q_{CS-I} = 1/2 q_{CS-II}$, were employed to investigate the cough strength effects on mucus clearance efficiency. Mucus clearance efficiency (see Fig. 7), air–mucus interface characteristics at selected planes C–C' and D–D' [see Figs. 12(b), 12(d), 13(b), and 13(d)], and local mucus distribution patterns (see Fig. 16) are visualized and discussed in this section.

The mucus clearance efficiencies shown in Fig. 7 imply that cough intensity plays a critical role in mucus clearance efficiency and mucus movement behaviors. Specifically, stronger cough (CS-II) can enhance the clearance efficiency, which is aligned with previous studies in idealized tracheas and bifurcated airways.^{17,37,41,42} The mucus

clearance efficiencies in the MT model with CS-II are 2.31 and 2.51 times higher than CS-I in two COPD severity levels, i.e., GOLD I and GOLD II, respectively (see Table III). In addition, the cough intensity can affect the mucus characteristics in the upper airways significantly [see Figs. 12(b), 12(d), 13(b), and 13(d)]. Figure 7 shows that a stronger cough can help COPD patients to carry the mucus from the trachea to the oral cavity. Such a phenomenon is more apparent in the upper airways with the thicker mucus condition. Indeed, the mucus initially in the trachea and the oropharynx (Z-1 and Z-2) moved into the oral cavity (Z-3). Therefore, mucus accumulations are formed in the oral cavity, which causes decreases in clearance efficiency in Z-3 (see Fig. 7). Furthermore, as shown in highlighted regions at C–C' and D–D' (see Figs. 8 and 9), the stronger cough can generate a thinner mucus layer due to the higher shear rate at the air–mucus interface that could be developed by a higher expiratory airflow velocity. Comparisons between Figs. 7(a) and 7(b) show that the mucus can overcome the gravity and viscous force in Z-1 when the expiratory airflow rate is higher than 6.59 L/s and avoid the mucus accumulation from Z-1 and Z-2 in this region with $\sigma = 1.0$ mm. This observation is supported by mucus volume fraction contours shown in Figs. 16(a) and 16(b).

However, the mucus in the right side of the supraglottic region and the oropharynx see the highlighted circled region in Figs. 14(c)

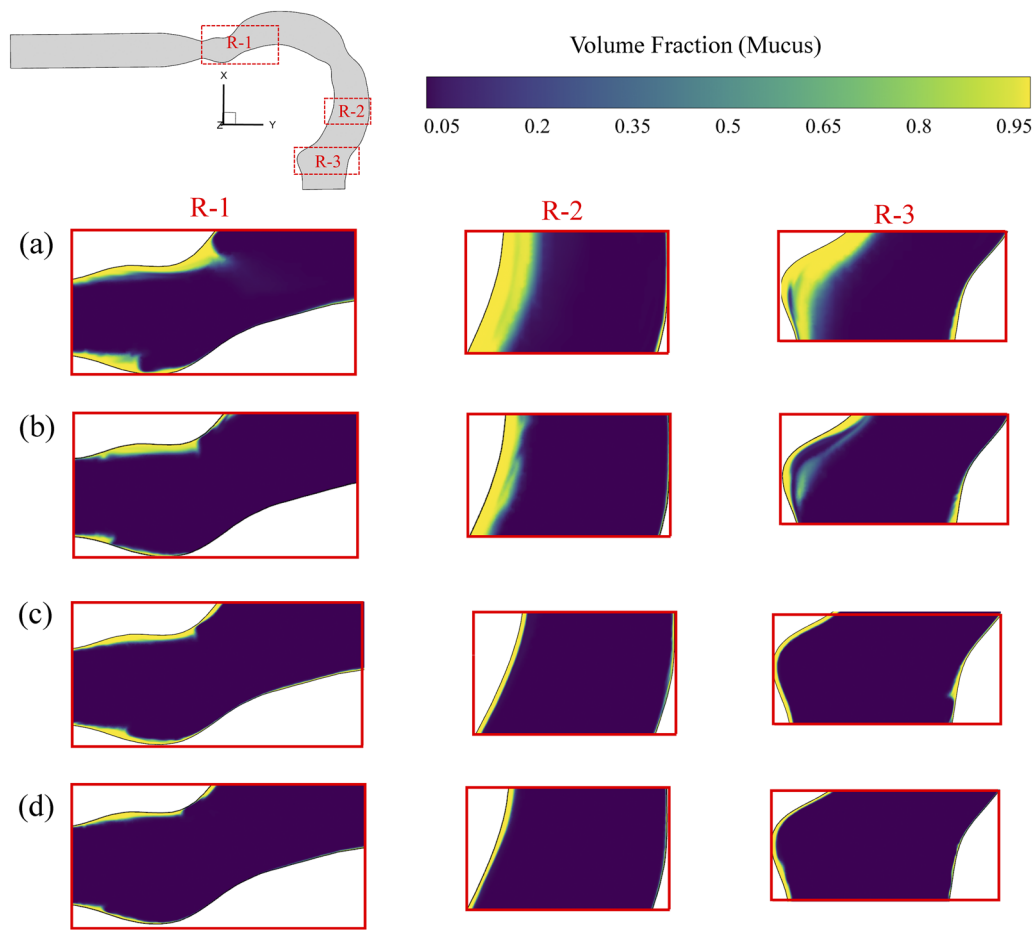


FIG. 16. Characteristics of non-Newtonian mucus in different regions ($t = 0.5126$ s): (a) $\sigma = 1.0$ mm and CS-I; (b) $\sigma = 1.0$ mm and CS-II; (c) $\sigma = 0.5$ mm and CS-I; and (d) $\sigma = 0.5$ mm and CS-II.

and 14(d), as well as R-1 and R-2 in Fig. 16, is cleared by the increased expiratory airflow. Such a fast removal could lead to direct exposure of the airway to inhaled air, toxicants, and virus-laden droplets without the protection of mucus, which may cause potential damages to the airway tissue and enhanced exposure risks. Thus, attention should be paid when the COPD patients develop intense cough strength to assist mucus clearance in pulmonary airways.

E. Transient effects of expiratory airflows on mucus clearance efficiency

During a single cough (see Fig. 4), the airflow-driven mucus clearance varies with time. Specifically, since the air velocity increases sharply to the maximum at $t = 0.09$ s and then decreases from 0.09 s to 0.40 s, the clearance efficiency (see Fig. 7) increases rapidly until $t = 0.09$ s, while the growth rate tends to slow down after $t = 0.40$ s. This can be explained by the fact that the larger shear stress produced by higher velocities around the cough peak can carry the mucus faster than when the airflow velocity is low. In all selected time stations (see Table III), i.e., $t = 0.05$ s, 0.09 s, 0.15 s, 0.20 s, 0.30 s, 0.40 s, and 0.5126 s, the mucus was cleared more efficiently with CS-II and

$\sigma = 1.0$ mm, which is also due to the high expiratory airflows (also see Secs. III C and III D). It is also worth mentioning that the clearance efficiencies reach a quasi-steady state after 0.3 s for both CS I and CS II (see Fig. 7). The negligible increase in clearance efficiency is due to the reduced mucus velocity after 0.3 s (see Table IV), determined by the reduced expiratory airflow velocity after 0.3 s (see Fig. 2).

Additionally, gravity also has a noticeable impact on the mucus transport and clearance, which can be observed from the clearance efficiency in Z-1 from $t = 0.40$ s to the end of the cough (see Table V and Fig. 7). Specifically, the mucus clearance efficiency in Z-1 decreases from $t = 0.40$ s to $t = 0.5126$ s. The decline in mucus clearance efficiency is because of the reversed flow from the upper airway to the trachea (i.e., from Z-2 back to Z-1) driven by the gravitational force. Therefore, reasonably intense expiratory airflow is needed to overcome gravity and to enhance the mucus clearance efficiency, although it will be difficult to achieve for severe COPD patients.

IV. CONCLUSIONS

The effects of the mucus viscosity model, cough strength, and mucus thickness on the airflow-driven COPD mucus clearance

TABLE V. Mucus clearance efficiency (%) in non-Newtonian fluid simulations at Z-1 during a single cough.

Conditions		Time (s)						
Mucus thickness (mm)	Cough strength	0.05	0.09	0.15	0.20	0.30	0.40	0.5126
1.0	CS-I	0.87	5.54	16.26	20.92	25.11	25.13	25.09
	CS-II	8.19	31.78	38.69	41.71	42.86	42.92	42.91
0.5	CS-I	0.61	0.64	0.86	0.94	1.05	1.08	1.07
	CS-II	0.71	2.04	5.59	7.18	7.78	7.80	7.79

process have been studied systematically in this paper using an experimentally validated VOF model. Quantitative conclusions are listed as follows:

- Using the Newtonian fluid viscosity model for mucus can significantly underpredict the mucus transport velocity and clearance, compared with the numerical results using a more realistic shear-thinning non-Newtonian fluid viscosity model. Therefore, it is highly recommended to model the mucus as a shear-thinning non-Newtonian fluid, rather than to simplify it as a Newtonian fluid. The conclusion should be further validated by experiments as future studies.
- The cough intensity plays a critical role in affecting mucus movement and clearance, i.e., the higher cough flow rate can increase the mucus clearance efficiency in the upper airway.
- Although higher mucus clearance efficiency is observed for a severe COPD condition with a thicker mucus layer, there is a possibility of mucus accumulation and obstruction in the upper airway for such a COPD condition if the cough is not strong enough, which will possibly cause further breathing difficulty.

V. LIMITATION OF THE STUDY AND FUTURE WORK

Mucus presents viscoelastic behaviors and shear-thinning characteristics, which were not considered in this study. Our long-term goal is to model the mucus viscoelasticity in computational lung aerosol dynamics studies. This study also did not simulate the cilia motion and the driven mucus transport phenomena explicitly. Accordingly, the feasible modeling strategy of the future work is to build a VOF plus Discrete Phase Model (VOF-DPM) with moving boundary conditions to explicitly model how cilia beats can drive the mucus, and track the air-mucus mixture, and trace the mucus clearance effect with the explicit tracking of inhaled particle transport in pulmonary airflow and mucus. The moving wall boundary conditions, i.e., the transient cilia beating velocities, can be applied, following the physiologically realistic beating patterns.^{13,75} The cilia velocity can be given in the form of a Fourier series.⁷⁶

SUPPLEMENTARY MATERIAL

See the [supplementary material](#) for the complete mesh independence test for the 3D straight tube for VOF model validation with benchmark experimental data.

AUTHORS' CONTRIBUTIONS

All authors contributed equally to this work.

ACKNOWLEDGMENTS

The use of Ansys software (Ansys Inc., Canonsburg, PA) as part of the Ansys-CBBL academic partnership is gratefully acknowledged. Some computational jobs were performed at the High-Performance Computing Center, Oklahoma State University, supported, in part, through the National Science Foundation (Grant No. OAC-1531128). The authors would like to thank Mrs. Pam Reynolds for constructive feedback and English language editing.

DATA AVAILABILITY

The data that support the findings of this study are available from the corresponding author upon reasonable request.

REFERENCES

- Y. Hu, S. Bian, J. Grotberg *et al.*, "A microfluidic model to study fluid dynamics of mucus plug rupture in small lung airways," *Biomicrofluidics* **9**, 044119 (2015).
- C. P. van der Schans, D. S. Postma, G. H. Koëter, and B. K. Rubin, "Physiotherapy and bronchial mucus transport," *Eur. Respir. J.* **13**, 1477–1486 (1999).
- R. Levy, D. B. Hill, M. G. Forest, and J. B. Grotberg, "Pulmonary fluid flow challenges for experimental and mathematical modeling," *Integr. Comp. Biol.* **54**, 985–1000 (2014).
- J. V. Fahy and B. F. Dickey, "Airway mucus function and dysfunction," *N. Engl. J. Med.* **363**, 2233–2247 (2010).
- D. B. Yeates, *Mucus Rheology* (Raven Press, Ltd., New York, 1990).
- D. B. Hill, P. A. Vasquez, J. Mellnik *et al.*, "A biophysical basis for mucus solids concentration as a candidate biomarker for airways disease," *PLoS One* **9**, e87681 (2014).
- S. K. Lai, Y.-Y. Wang, D. Wirtz, and J. Hanes, "Micro- and macrorheology of mucus," *Adv. Drug Delivery Rev.* **61**, 86–100 (2009).
- P. J. Basser, T. A. McMahon, and P. Griffith, "The mechanism of mucus clearance in cough," *J. Biomech. Eng.* **111**, 288–297 (1989).
- M. S. Quraishi, N. S. Jones, and J. Mason, "The rheology of nasal mucus: A review," *Clin. Otolaryngol.* **23**, 403–413 (1998).
- G. B. Wallis, *One Dimensional Two-Phase Flow* (McGraw-Hill, New York, 1969).
- N. Sanders, C. Rudolph, K. Braeckmans, S. C. De Smedt, and J. Demeester, "Extracellular barriers in respiratory gene therapy," *Adv. Drug Delivery Rev.* **61**, 115–127 (2009).
- J. Leal, H. D. C. Smyth, and D. Ghosh, "Physicochemical properties of mucus and their impact on transmucosal drug delivery," *Int. J. Pharm.* **532**, 555–572 (2017).
- D. J. Smith, E. A. Gaffney, and J. R. Blake, "Modelling mucociliary clearance," *Respir. Physiol. Neurobiol.* **163**, 178–188 (2008).
- C. Karamaoun, B. Sobac, B. Mauroy, A. Van Muylem, and B. Haut, "New insights into the mechanisms controlling the bronchial mucus balance," *PLoS One* **13**, e0199319 (2018).
- Y. Zheng, *Liquid Plug Dynamics in Pulmonary Airways* (UMI Dissertation Publishing, 2011).

- ¹⁶B. K. Rubin, "Physiology of airway mucus clearance," *Respir. Care* **47**, 761–768 (2002).
- ¹⁷S. Ren, W. Li, L. Wang *et al.*, "Numerical analysis of airway mucus clearance effectiveness using assisted coughing techniques," *Sci. Rep.* **10**, 2030 (2020).
- ¹⁸M. L. Groth, K. Macri, and W. M. Foster, "Cough and mucociliary transport of airway particulate in chronic obstructive lung disease," *Ann. Occup. Hyg.* **41**, 515–521 (1997).
- ¹⁹C. P. van der Schans, "Bronchial mucus transport," *Respir. Care* **52**, 1150–1158 (2007).
- ²⁰G. V. Emmanouil, *Environmental and Occupational Epidemiology Principles. Environmental Exposures and Human Health Challenges* (IGI Global, Hershey, PA, USA, 2019), pp. 147–157.
- ²¹R. J. Thomas, "Particle size and pathogenicity in the respiratory tract," *Virulence* **4**, 847–858 (2013).
- ²²M. Zanin, P. Baviskar, R. Webster, and R. Webby, "The interaction between respiratory pathogens and mucus," *Cell Host Microbe* **19**, 159–168 (2016).
- ²³C. K. Tran and E. D. Kuempel, "Biologically based lung dosimetry and exposure-dose-response models for poorly soluble inhaled particles," in *Particle Toxicology*, edited by P. Borm and K. Donaldson (CRC Press, OH, 2007), pp. 351–386.
- ²⁴J. Yang, E. K. Kim, H. J. Park, A. McDowell, and Y.-K. Kim, "The impact of bacteria-derived ultrafine dust particles on pulmonary diseases," *Exp. Mol. Med.* **52**, 338–347 (2020).
- ²⁵J. E. Salvaggio, "Inhaled particles and respiratory disease," *J. Allergy Clin. Immunol.* **94**, 304–309 (1994).
- ²⁶R. D. Turner and G. H. Bothamley, "Cough and the transmission of tuberculosis," *J. Infect. Dis.* **211**, 1367–1372 (2014).
- ²⁷M. Richardson, "The physiology of mucus and sputum production in the respiratory system," *Nurs. Times* **99**, 63–64 (2003).
- ²⁸J. M. Samet and P.-W. Cheng, "The role of airway mucus in pulmonary toxicology," *Environ. Health Perspect.* **102**, 89–103 (1994).
- ²⁹B. Button and R. C. Boucher, "Role of mechanical stress in regulating airway surface hydration and mucus clearance rates," *Respir. Physiol. Neurobiol.* **163**, 189–201 (2008).
- ³⁰P. L. Shah, S. F. Scott, R. A. Knight, C. Marriott, C. Ranasinha, and M. E. Hodson, "In vivo effects of recombinant human DNase I on sputum in patients with cystic fibrosis," *Thorax* **51**, 119–125 (1996).
- ³¹B. K. Rubin, O. Ramirez, and J. A. Ohar, "Iodinated glycerol has no effect on pulmonary function, symptom score, or sputum properties in patients with stable chronic bronchitis," *Chest* **109**, 348–352 (1996).
- ³²J. G. Zayas, G. C. W. Man, and M. King, "Tracheal mucus rheology in patients undergoing diagnostic bronchoscopy: Interrelations with smoking and cancer," *Am. Rev. Respir. Dis.* **141**, 1107–1113 (1990).
- ³³A. Jeanneret-Grosjean, M. King, M. C. Michoud, H. Liote, and R. Amyot, "Sampling technique and rheology of human tracheobronchial mucus," *Am. Rev. Respir. Dis.* **137**, 707–710 (1988).
- ³⁴B. K. Rubin, O. Ramirez, J. G. Zayas, B. Finegan, and M. King, "Collection and analysis of respiratory mucus from subjects without lung disease," *Am. Rev. Respir. Dis.* **141**, 1040–1043 (1990).
- ³⁵E. Puchelle, J. M. Zahm, and C. Duvivier, "Spinability of bronchial mucus. Relationship with viscoelasticity and mucous transport properties," *Biorheology* **20**, 239–249 (1983).
- ³⁶M. J. Dulfano, K. Adler, and W. Philippoff, "Sputum viscoelasticity in chronic bronchitis," *Am. Rev. Respir. Dis.* **104**, 88–98 (1971).
- ³⁷C. S. Kim, C. R. Rodriguez, M. A. Eldridge, and M. A. Sackner, "Criteria for mucus transport in the airways by two-phase gas-liquid flow mechanism," *J. Appl. Physiol.* **60**, 901–907 (1986).
- ³⁸G. B. Wallis and J. E. Dodson, "The onset of slugging in horizontal stratified air-water flow," *Int. J. Multiphase Flow* **1**, 173–193 (1973).
- ³⁹R. R. Rajendran and A. Banerjee, "Mucus transport and distribution by steady expiration in an idealized airway geometry," *Med. Eng. Phys.* **66**, 26–39 (2019).
- ⁴⁰C. Paz, E. Suárez, J. Vence, and A. Cabarcos, "Analysis of the volume of fluid (VOF) method for the simulation of the mucus clearance process with CFD," *Comput. Methods Biomech. Biomed. Eng.* **22**, 547–566 (2019).
- ⁴¹C. S. Kim, A. J. Iglesias, and M. A. Sackner, "Mucus clearance by two-phase gas-liquid flow mechanism: Asymmetric periodic flow model," *J. Appl. Physiol.* **62**, 959–971 (1987).
- ⁴²C. S. Kim, M. A. Greene, S. Sankaran, and M. A. Sackner, "Mucus transport in the airways by two-phase gas-liquid flow mechanism: Continuous flow model," *J. Appl. Physiol.* **60**, 908–917 (1986).
- ⁴³M. King, G. Brock, and C. Lundell, "Clearance of mucus by simulated cough," *J. Appl. Physiol.* **58**, 1776–1782 (1985).
- ⁴⁴R. Camassa, M. G. Forest, L. Lee, H. R. Ogrskey, and J. Olander, "Ring waves as a mass transport mechanism in air-driven core-annular flows," *Phys. Rev. E* **86**, 066305 (2012).
- ⁴⁵Y. Feng, C. Kleinstreuer, N. Castro, and A. Rostami, "Computational transport, phase change and deposition analysis of inhaled multicomponent droplet-vapor mixtures in an idealized human upper lung model," *J. Aerosol Sci.* **96**, 96–123 (2016).
- ⁴⁶Y.-S. Cheng, Y. Zhou, and B. T. Chen, "Particle deposition in a cast of human oral airways," *Aerosol Sci. Technol.* **31**, 286–300 (1999).
- ⁴⁷C. W. Hirt and B. D. Nichols, "Volume of fluid (VOF) method for the dynamics of free boundaries," *J. Comput. Phys.* **39**, 201–225 (1981).
- ⁴⁸M. Ishii and T. Hibiki, *Thermo-Fluid Dynamics of Two-Phase Flow* (Springer, New York, NY, 2011).
- ⁴⁹C. Paz, E. Suárez, O. Parga, and J. Vence, "Glottis effects on the cough clearance process simulated with a CFD dynamic mesh and Eulerian wall film model," *Comput. Methods Biomech. Biomed. Eng.* **20**, 1326–1338 (2017).
- ⁵⁰C. Paz, E. Suárez, and J. Vence, "CFD transient simulation of the cough clearance process using an Eulerian wall film model," *Comput. Methods Biomech. Biomed. Eng.* **20**, 142–152 (2017).
- ⁵¹D. Sanchez, L. Hume, R. Chatelin, and P. Poncet, "Analysis of 3D non-linear Stokes problem coupled to transport-diffusion for shear-thinning heterogeneous microscale flows, applications to digital rock physics and mucociliary clearance," *ESAIM: Math. Modell. Numer. Anal.* **53**, 1083 (2018).
- ⁵²R. A. Cone, "Barrier properties of mucus," *Adv. Drug Delivery Rev.* **61**, 75–85 (2009).
- ⁵³J. U. Brackbill, D. B. Kothe, and C. Zemach, "A continuum method for modeling surface tension," *J. Comput. Phys.* **100**, 335–354 (1992).
- ⁵⁴R. Hamed and J. Fiegel, "Synthetic tracheal mucus with native rheological and surface tension properties," *J. Biomed. Mater. Res. A* **102**, 1788–1798 (2014).
- ⁵⁵J. A. Clements, E. S. Brown, and R. P. Johnson, "Pulmonary surface tension and the mucus lining of the lungs: Some theoretical considerations," *J. Appl. Physiol.* **12**, 262–268 (1958).
- ⁵⁶F. Y. Kafka and E. B. Dussan, "On the interpretation of dynamic contact angles in capillaries," *J. Fluid Mech.* **95**, 539–565 (1979).
- ⁵⁷R. P. Mahajan, P. Singh, G. E. Murty, and A. R. Aitkenhead, "Relationship between expired lung volume, peak flow rate and peak velocity time during a voluntary cough manoeuvre," *Br. J. Anaesth.* **72**, 298–301 (1994).
- ⁵⁸G. C. Leiner, S. Abramowitz, M. J. Small, and V. B. Stenby, "Cough peak flow rate," *Am. J. Med. Sci.* **251**, 211–214 (1966).
- ⁵⁹J. K. Gupta, C.-H. Lin, and Q. Chen, "Flow dynamics and characterization of a cough," *Indoor Air* **19**, 517–525 (2009).
- ⁶⁰J. K. Gupta, C.-H. Lin, and Q. Chen, "Transport of expiratory droplets in an aircraft cabin," *Indoor Air* **21**, 3–11 (2011).
- ⁶¹N. Dudalski, A. Mohamed, S. Mubareka, R. Bi, C. Zhang, and E. Savory, "Experimental investigation of far-field human cough airflows from healthy and influenza-infected subjects," *Indoor Air* **30**, 966 (2020).
- ⁶²Y. Feng, T. Marchal, T. Sperry, and H. Yi, "Influence of wind and relative humidity on the social distancing effectiveness to prevent COVID-19 airborne transmission: A numerical study," *J. Aerosol Sci.* **147**, 105585 (2020).
- ⁶³L. Yang, X. Li, Y. Yan, and J. Tu, "Effects of cough-jet on airflow and contaminant transport in an airliner cabin section," *J. Comput. Multiphase Flows* **10**, 72–82 (2017).
- ⁶⁴A. F. I. Dincer, *Exergy for A Better Environment and Improved Sustainability 1: Fundamentals* (Springer International Publishing, Switzerland, AG, 2018).
- ⁶⁵F. L. Ramos, J. S. Krahnke, and V. Kim, "Clinical issues of mucus accumulation in COPD," *Int. J. Chronic Obstruct. Pulm. Dis.* **9**, 139–150 (2014).
- ⁶⁶D. Picchi, P. Poesio, A. Ullmann, and N. Brauner, "Characteristics of stratified flows of Newtonian/non-Newtonian shear-thinning fluids," *Int. J. Multiphase Flow* **97**, 109–133 (2017).

- ⁶⁷B. Mauroy, C. Fausser, D. Pelca, J. Merckx, and P. Flaud, "Toward the modeling of mucus draining from the human lung: Role of the geometry of the airway tree," *Phys. Biol.* **8**, 056006 (2011).
- ⁶⁸R. Camassa, M. G. Forest, L. Lee, H. R. Ogrosky, and J. Olander, "Ring waves as a mass transport mechanism in air-driven core-annular flows," *Phys. Rev. E* **86**(6 Pt 2), 066305 (2012).
- ⁶⁹R. Chatelin, D. Anne-Archard, M. Murris-Espin, M. Thiriet, and P. Poncet, "Numerical and experimental investigation of mucociliary clearance breakdown in cystic fibrosis," *J. Biomech.* **53**, 56–63 (2017).
- ⁷⁰Z. Żolek-Tryznowska, "6—Rheology of printing inks," in *Printing on Polymers*, edited by J. Izdebska and S. Thomas (William Andrew Publishing, 2016), pp. 87–99.
- ⁷¹G. D'Avino, "8—Numerical simulations of viscoelastic suspension fluid dynamics," in *Rheology of Non-Spherical Particle Suspensions*, edited by F. Chinesta and G. Ausias (Elsevier, 2015), pp. 235–280.
- ⁷²A. N. Antonov and E. N. Bondarev, "Approximate method for calculating turbulent boundary layer with positive pressure gradient," *Fluid Dyn.* **3**, 41–42 (1968).
- ⁷³M. B. D. Gavião and A. V. d. Bilt, "Salivary secretion and chewing: Stimulatory effects from artificial and natural foods," *J. Appl. Oral Sci.* **12**, 159–163 (2004).
- ⁷⁴J. Hewitt, L. Smeeth, C. J. Bulpitt, A. J. Tulloch, and A. E. Fletcher, "Respiratory symptoms in older people and their association with mortality," *Thorax* **60**, 331–334 (2005).
- ⁷⁵S. Gueron and K. Levit-Gurevich, "Computation of the internal forces in cilia: Application to ciliary motion, the effects of viscosity, and cilia interactions," *Biophys. J.* **74**, 1658–1676 (1998).
- ⁷⁶G. R. Fulford and J. R. Blake, "Muco-ciliary transport in the lung," *J. Theor. Biol.* **121**, 381–402 (1986).